Energy, Mines and Resources Canada
Énergie, Mines et Ressources Canada

CANMET
Canada Centre for Mineral and Energy Technology
Centre canadien de la technologie des minéraux et de l'énergie

HYDRODYNAMIC BEHAVIOUR OF GAS-LIQUID TWO-PHASE FLOWS AT ELEVATED TEMPERATURES AND PRESSURES

D.D.S. Liu, D.J. Patmore and J.J. Lipsett

February 1985

For presentation at the 35th Canadian Chemical Engineering Conference at Calgary, Alberta, October 6-9, 1985 and for publication in proceedings

ENERGY RESEARCH PROGRAM
ENERGY RESEARCH LABORATORIES
DIVISION REPORT ERP/ERL 85-21 (OPJ)

HYDRODYNAMIC BEHAVIOUR OF GAS-LIQUID TWO-PHASE FLOWS AT ELEVATED TEMPERATURES AND PRESSURES

D.D.S. Liu*, D.J. Patmore* and J.J. Lipsett+

* Energy Research Laboratories, CANMET, EMR, Ottawa, Ontario, Canada
+ AECL-CRNL, Chalk River, Ontario, Canada

ABSTRACT

A single-beam gamma-ray densitometer capable of precise vertical and horizontal scanning has been developed for the study of hydrodynamic phenomena in gas/liquid and gas/liquid/solid multi-phase flow columns. Studies were made on thick-walled reactors at elevated temperatures and pressures for hydrogen/organic liquid systems. Under these conditions, methods that rely on the insertion of sensors cannot be employed easily.

Time dependent gamma-ray attenuation caused by gas bubbles passing through the fluid was measured at different positions and under various conditions in two vertical continuous-flow columns. In addition to time averaged attenuation recorded by a single-channel scaler for measurement of mean local voidages, probability density distributions (PDD) were measured in order to investigate the homogeneity of bubble distributions. A statistical model was developed to deconvolute the PDD function and to correlate them with the instantaneous voidage. Analyses show that this technique is a powerful tool for the determination of void fraction and flow regime.

INTRODUCTION

Many multi-phase flow columns are being used in petroleum refineries and chemical plants operating at elevated temperatures and pressures. Although the hydrodynamic behaviour of multi-phase systems including gas/liquid and gas/liquid/solid flows has been studied extensively at or near ambient conditions, information on systems operated at high pressures and temperatures is scarce.

CANMET's Energy Research Laboratories has been involved in the development of processes for upgrading bitumen, heavy oils and coal slurries for many years (1-3). As part of the fundamental research in support of such process development, the hydrodynamic behaviour of multi-phase flow at elevated temperatures and pressures is being studied.

Processes operating at high temperatures and pressures require thick-walled vessels. At these conditions, methods requiring the insertion of probes to determine hydrodynamic behaviours are difficult to employ. Therefore, non-invasive techniques were sought resulting in the development of a single, narrow-beam gamma-ray densitometer with digital time series analysis of the signals (4). Operating

principles and experimental results are described.

BACKGROUND

The attenuation of a gamma-ray beam follows Beer's equation:

$$N = N_o \exp[-(\mu/A)\ V] \qquad \text{Eq. 1}$$

where: A = cross-sectional area of the beam (cm^2)
N = detected counting rate (counts/s)
N_o = counting rate when column is empty (counts/s)
V = volume of the material (cm^3)
μ = attenuation coefficient (cm^{-1})

For gas/liquid two-phase flow, attenuation due to gas is much less than that of the liquid and therefore can be neglected even at high pressure. The volumetric fraction of liquid in the control volume, V_c, as a function of time can be written as:

$$V_L = (V_c / \theta) \int_0^{\theta} [1 - e(t)]dt \qquad \text{Eq. 2}$$

where: $e(t)$ = the time dependent voidage within the control volume
θ = the counting period (s)

If we define N_E and N_F as count rates for the attenuation when the column is empty or full of liquid Eq. 1 and 2 show the count rates as constant.

The count rate, N_t, at time, t, is related to the void fraction within the measuring volume at the time of measuring by:

$$e(t) = \ln(N_t/N_F)/\ln(N_E/N_F) \qquad \text{Eq. 3}$$

The sampling period, θ, used in Eq. 2 depends on the information required. For a small sampling period with continuously repetitive recording, the voidage as a function of time can be obtained in order to identify the flow regime, whereas a long sampling time allows a direct measurement of mean voidage.

Equation 2 allows the determination of the temporal mean void fraction within the measuring control volume, V_c:

$$e(t) = V_L(t)/V_c \qquad \text{Eq. 4}$$

When a two-phase flow contains homogeneous bubbles with bubble cross-sections (diameters) smaller than that of the gamma-ray beam, the voidage in the control volume [e(t)] is identical to that of the cross-section of the column. However, when the gas flows through a central core (slug or annular flow), the column cross-sectional voidage is related to the control volume voidage by

$$e_{slug}(t) = [e(t)]^2 \qquad \text{Eq. 5}$$

A few methods have been developed to overcome this ambiguity including a single beam with multiple scanning (5), multiple-beam densitometry (6,7) and tomographic techniques (8,9). Most are unsuitable for our applications.

A method involving the analysis of PDD functions of the sampled time functions observed by using a single-beam gamma ray has been developed to overcome this difficulty (4).

EXPERIMENTAL AND RESULTS

A 2 Ci Cs^{137} (0.662 MeV) source radiating across a diameter of a cylindrical vessel was used. A NaI(Tl) detector located on the other side of the column was used to detect gamma-ray photons. The gamma ray is confined to a well defined narrow beam geometry by collimators placed in front of both source and detector. A single-channel scaler and a multi-channel analyzer (MCA) were then used to register count rates and PDD functions.

Two vessels were used. One is made of plexiglass for gamma-ray measurements and photography at perpendicular directions using a nitrogen/water bubble column. The other is a thick-walled stainless steel vessel for simulating multi-phase flow at elevated temperatures and pressures.

The source and detector are mounted on a metal plate thus the relative positions are fixed. The plate is vertically and horizontally movable and is controlled by a specialized logic to precisely locate the desired measuring volume position. Figure 1 shows a photograph of the scanner.

Figure 2 shows nitrogen/water bubbling phenomena studied at ambient conditions. Figures 3 to 6 show histograms of their count rates. Figures 3 and 4 show the original spectra recorded using a MCA. Noises due to the detector (see next section) are clearly visible. Distinguishable peaks were observed when large bubbles passed through the gamma ray when the spectra were smoothed (Fig. 5 and 6).

The PDD of the time function is a plot of the number of occurrences of a given count rate versus that count rate which is proportional to the channel number of the MCA. Figures 7 to 9 show the PDD functions corresponding to the flows shown in Fig. 2.

Qualitative applications of the PDD have been reported for multi-phase flow studies by using X-ray techniques (10,11) and by surface pressure measurements (12,13). The method is extended here for quantitative studies.

Hydrogen/heavy gas-oil (zerice) and hydrogen/heavy oil two-phase upward flow systems were measured by the gamma-ray scanner at various pressures and temperatures through the thick-walled steel vessel. Examples of some PDD functions are shown in Fig. 10 to 13.

DISCUSSION

VISUALIZATION OF BUBBLES BY GAMMA-RAY ATTENUATION MEASUREMENTS

Measurements from the cold model serve as good examples to illustrate the technique. The PDD spectrum line broadening due to detector noise for a constant count rate is a Poisson distribution (14). When the count rate is sufficiently high, the distribution approaches a Gaussian distribution with a full width at half maximum (FWHM) given by:

$$FWHM = [N/(2\tau)]^{1/2} \qquad \text{Eq. 6}$$

when a ratemeter with a time constant, τ, is used.

The PDD observed for fine bubbly two-phase flow follow Eq. 6 well (Fig. 7). However, when the voidage is a time variant phenomenon, the PDD functions are further broadened by the inhomogeneity of the bubble distribution (Fig. 8); also, when large gas slugs appear, an extra peak at high counting rate (near N_E) is observed (Fig. 8 and 9). The area fraction of this peak is the fraction of time during the measurement when the flow is "annular" at the plane of the gamma ray.

Since the attenuation by the vessel is much larger than that due to the fluid, the resolution of PDD function cannot be high. The amplitude of the PDD at a given channel (counting rate) consists of contributions from multiple steady PDD peaks. This is confirmed by examination of photographs (Fig. 2) and histograms (Fig. 3 to 6) which show that bubbles and slugs appear in groups. Based on these observations, a deconvolution model is developed.

The deconvolution, through an iterative least square process, determined that the PDD under our process conditions contained discrete features. These are well separated by their associated count rates. Thus the PDD resembled X-ray spectra where the statistical noise caused by the count rate was analogous to spectrum line broadening due to detector noise. An example is given in Fig. 9 in which the deconvoluted peaks are shown by vertical bars.

The count rate and area of the ith peak are defined as N_i and A_i, respectively. The probability of observing a count rate, N_i, is:

$$P_i = A_i \,/\, (\sum A_j) \qquad \text{Eq. 7}$$

where the denominator sums all peaks in the PDD.

The voidage for this peak, $e_i(t)$, can be determined by either Eq. 3 or 5 depending on whether the count rate is attributed to bubbly or slug flow. This can be easily determined from histograms similar to those shown in Fig. 4 to 6.

The overall mean voidage can then be determined by:

$$e_{ave}(t) = \sum e_j(t)\ P_j \qquad \text{Eq. 8}$$

Equation 8 is the first moment of the PDD function.

This model is similar to the use of the residence time distribution function to derive first moment parameters in chemical reaction engineering.

EFFECT OF PRESSURE AND TEMPERATURE ON VOIDAGE

Systems including nitrogen/heavy gas-oil, hydrogen/heavy oil and hydrogen/heavy oil/solid at various conditions have been studied. Some examples for hydrogen/heavy oil are given here.

Figures 10 and 11 show the PDD functions observed at 200°C, for flows at P = 1.38 MPa, U_g = 2.02 cm/s and P = 10.35 MPa, U_g = 1.66 cm/s (U_g = superficial gas velocity). The bubble size distributions for these runs are similar and there are only small differences in mean voidage at the same gas velocity. The long tails at high count rates in the PDD functions indicate the appearance of discrete bubbles larger than the cross-sectional area of the gamma-ray beam. Although photographs could not be obtained because a thick-walled steel vessel was used, the behaviour is expected to be similar to that shown in Fig. 2b as indicated by the similarity in the observed PDD functions in both cases (Fig. 8, 10 and 11).

When the temperature was increased to 300°C, the number of large bubbles were reduced significantly as shown in Fig. 12 by the shortening of the tail of the PDD function in comparison with those shown in Fig. 10 and 11. On the other hand, the count rate of the major peak increased significantly in comparison with that observed at 200°C for a similar superficial gas velocity. This indicates that the bubble size distribution became narrower.

A further increase in temperature to 350°C caused the large bubbles to disappear almost completely as shown by the absence of a tail on the PDD function (Fig. 13). Also, the mean voidage increased further as indicated by the shift in peak position to an even higher count rate than that at 300°C. The PDD function (Fig. 13) was quite symmetrical and had an FWHM close to the theoretical value predicted by Eq. 6 indicating that the bubble distribution was very homegeneous and most of the bubbles were smaller than the cross section of the gamma-ray beam used (diameter < 0.637 cm).

CONCLUSIONS

The effect of pressure on void fraction is significant only for systems at relatively low pressure (<1 MPa) where the hydrostatic head affects the gas density, provided there is no significant change in other parameters.

The observed dominating effect of temperature on void fraction is presumably due to changes in rheological properties and surface tension of the

liquid, with the result that only fine bubbles are observed at high temperature. This explains why very large void fractions have been observed at high temperatures and pressures at ERL and elsewhere (15,16).

REFERENCES

1. Lunin, G., Silva, A.E., and Denis, J.M. "The CANMET hydrocracking process (Upgrading of Cold Lake heavy oil)", 30th Can. Chem. Eng. Conf., Edmonton, Alberta, October 1980.
2. Menzies, M.A., Silva, A.E. and Denis, J.M. "Hydrocracking without catalysis upgrades heavy oil", Chem. Engng., p.46, February 1981.
3. Fouda, S.A., Ikura, M. and Kelly, J.F. "Coprocessing of Canadian lignites and bitumen", AIChE Spring National Meeting, Houston, Texas, March 1985.
4. Lipsett, J.J., Noble, R.D. and Liu, D.D.S. "Time series analysis of gamma densitometry signals", Accepted for publication in Nuclear Instruments and Methods.
5. Gardner, R.P. and Ely, R.L. "Radioisotope measurement analysis in engineering", N.Y., Reinhold Publishing Corp., pp 336-42, 1967.
6. Kondic, N.D. and Lassahn, G.D. "Noninstrusive density distribution measurement in dynamic high temperature systems", 24th Int. Instr. Sym., Albuquerque, NM, 1978.
7. Banerjee, T.R., Heidrik, T.R., Saltvold, J.R. and Flemons, R.S. "Measurement of void fraction and mass velocity in transient two-phase flow", Transient Two-Phase Flow, Proceedings of the CSNI Specialists Meeting, August 1976, Toronto (Editors Banerjee, S. and Weaver, K.R.) Atomic Energy of Canada Limited Report AECL-2, pp 789-832, 1978.
8. Fincke, J.R. "Tomographic reconstruction of the time-averaged density distribution in two-phase flow", EGG-M-11481, 1982.
9. Tonner, P.D. and Taylor, T. "Region-of-interest tomography", Atomic Energy of Canada Limited Report AECL-8560, 1985.
10. Jones, O.C. and Zuber, N. "The interrelation between void fractions and flow patterns in two-phase flow", Int. J. Multiphase Flow, **2**, 273, 1975.
11. Albrecht, R.W., Crowe, R.D., Dailey, D.J., Damborg, M.J. and Kosaly, G. "Measurement of two phase flow properties using the nuclear reactor instrument", Progress in Nuclear Engergy, **9**, 37, 1982.
12. Hubbard, M.G. and Dukler, A.E. "The characterization of flow regimes for horizontal two-phase flow: I. Statistical analysis of wall pressure fluctuations", Proceedings of the 1966 Heat Transfer and Fluid Mechanics Institute (Editors Saad, M.A. and Miller, J.A.) pp 100-121, Standford Uni. Press, Palo Alto, CA, 1977.
13. Matsui, G. "Identification of flow regimes in vertical gas-liquid two-phase flow using differential pressure fluctuations", Int. J. Multiphase Flow, **10**, 711, 1984.
14. Evans, R.D. "The atomic nucleus", N.Y., McGraw-Hill, 1955.
15. Blum, D.B. and Toman, J.T. "Three-phase fluidization in a liquid phase methanator", AIChE Sym. Ser. (Formerly CEPSA) - CISTI, **73**, 115, 1977.
16. Tarmy, B.L., Chang, M., Coulaloglou, C.A. and Ponzi, P.R. "The three phase

hydrodynamic characteristics of the EDS coal liquefaction reactors: Their development and use in reactor scaleup", 8th Int. Sym. Chem. Reaction Eng., **87**, 303, 1984.

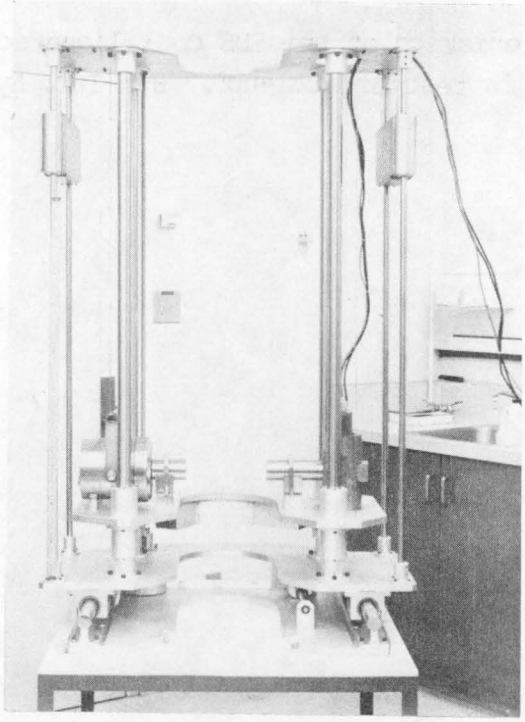

Fig. 1 - CANMET's gamma-ray densitometer for hydrodynamic studies

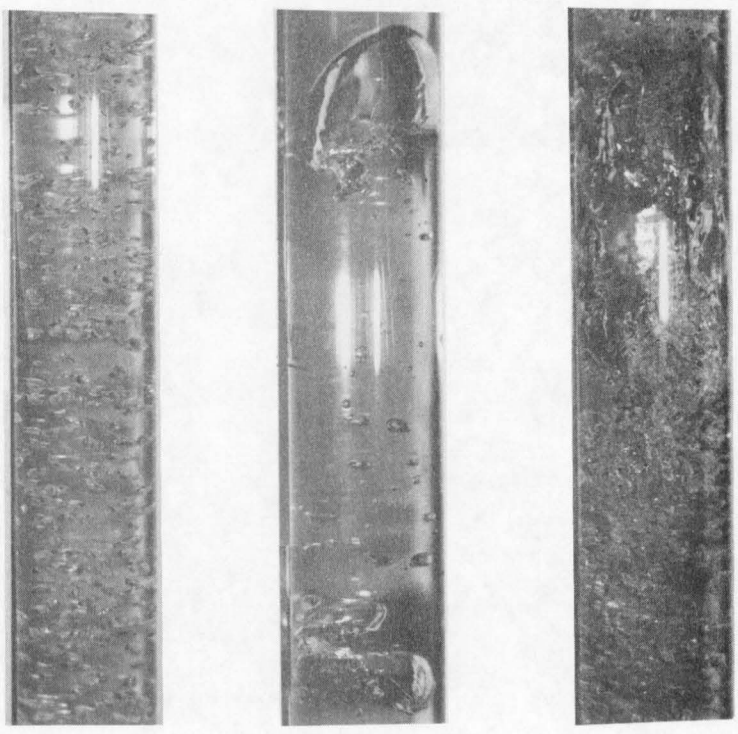

(a) (b) (c)

Fig. 2 - Nitrogen-water bubble column patterns
a. Fine bubbles (U_g = 2.0 cm/s; gas through a distributor)
b. Independent bubbles (U_g = cm/s; single sparger)
c. Slug flow (U_g = cm/s; single sparger)

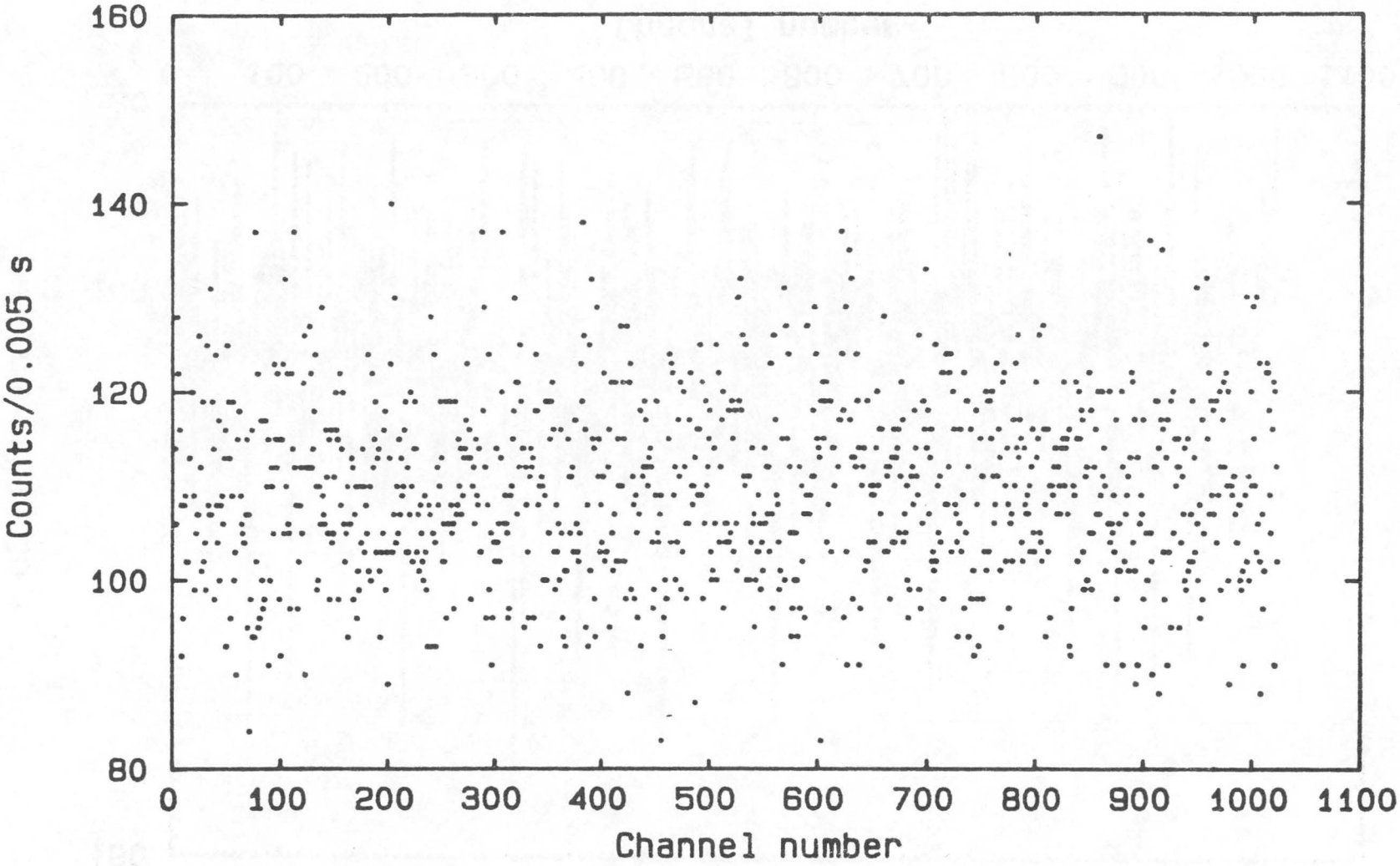

Fig. 3 - Histogram of gamma-ray interrogation count rate observed for fine bubble distribution flow shown in Fig. 2a

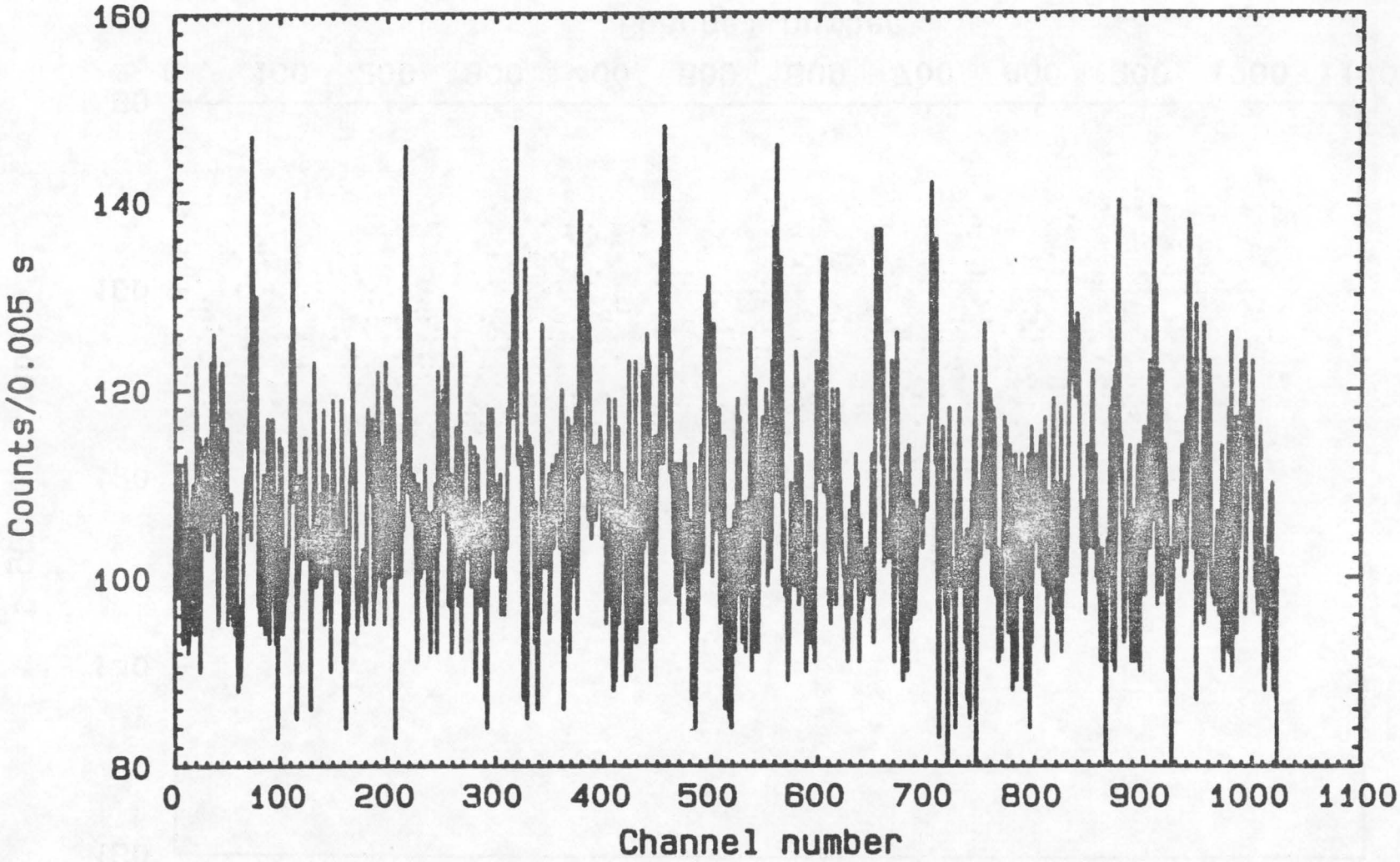

Fig. 4 - Histogram of gamma-ray interrogation count rate oberved for independent bubbles shown in Fig. 2b

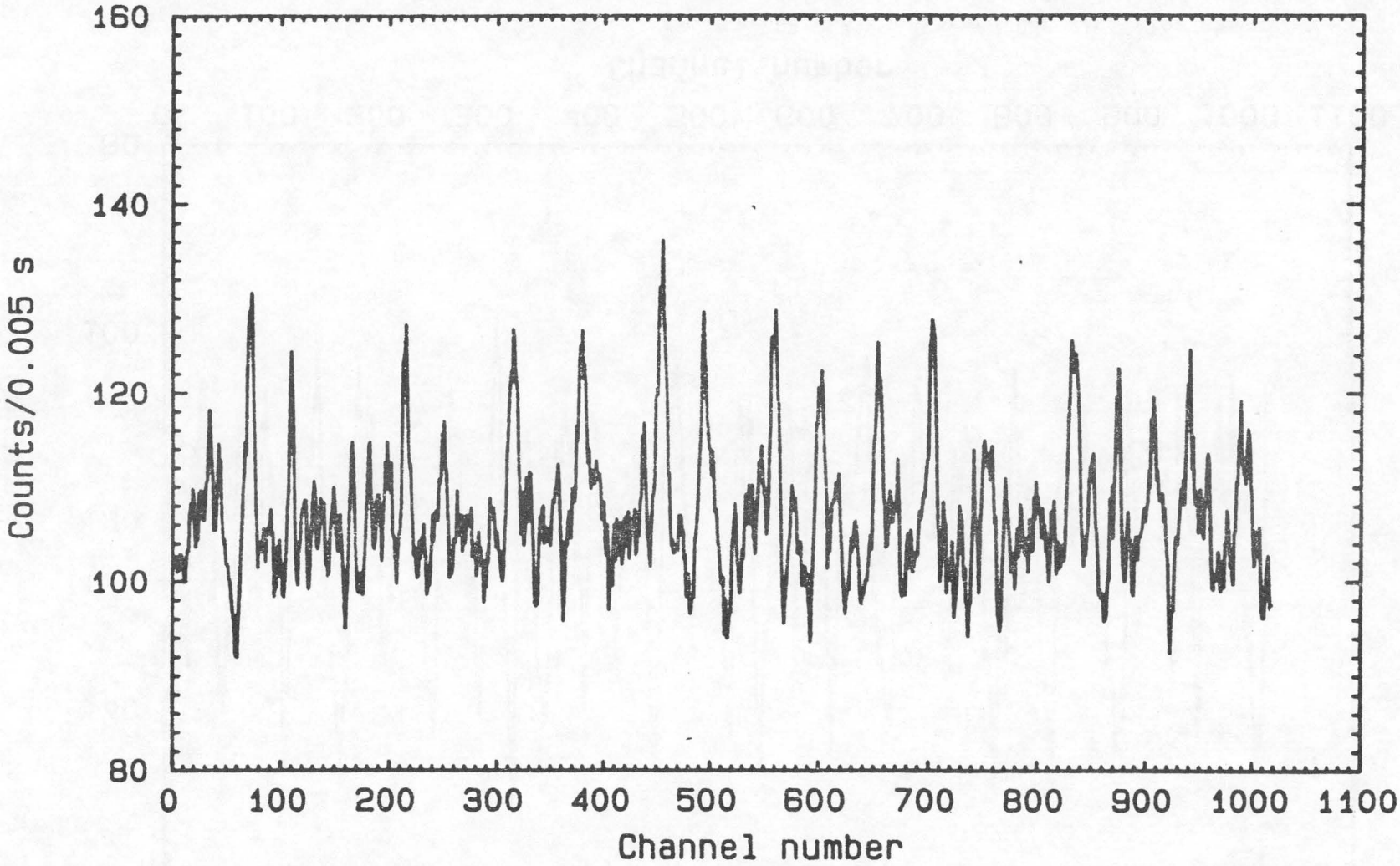

Fig. 5 - Smoothed histogram of gamma-ray interrogation count rate for those shown in Fig. 2b and Fig. 4

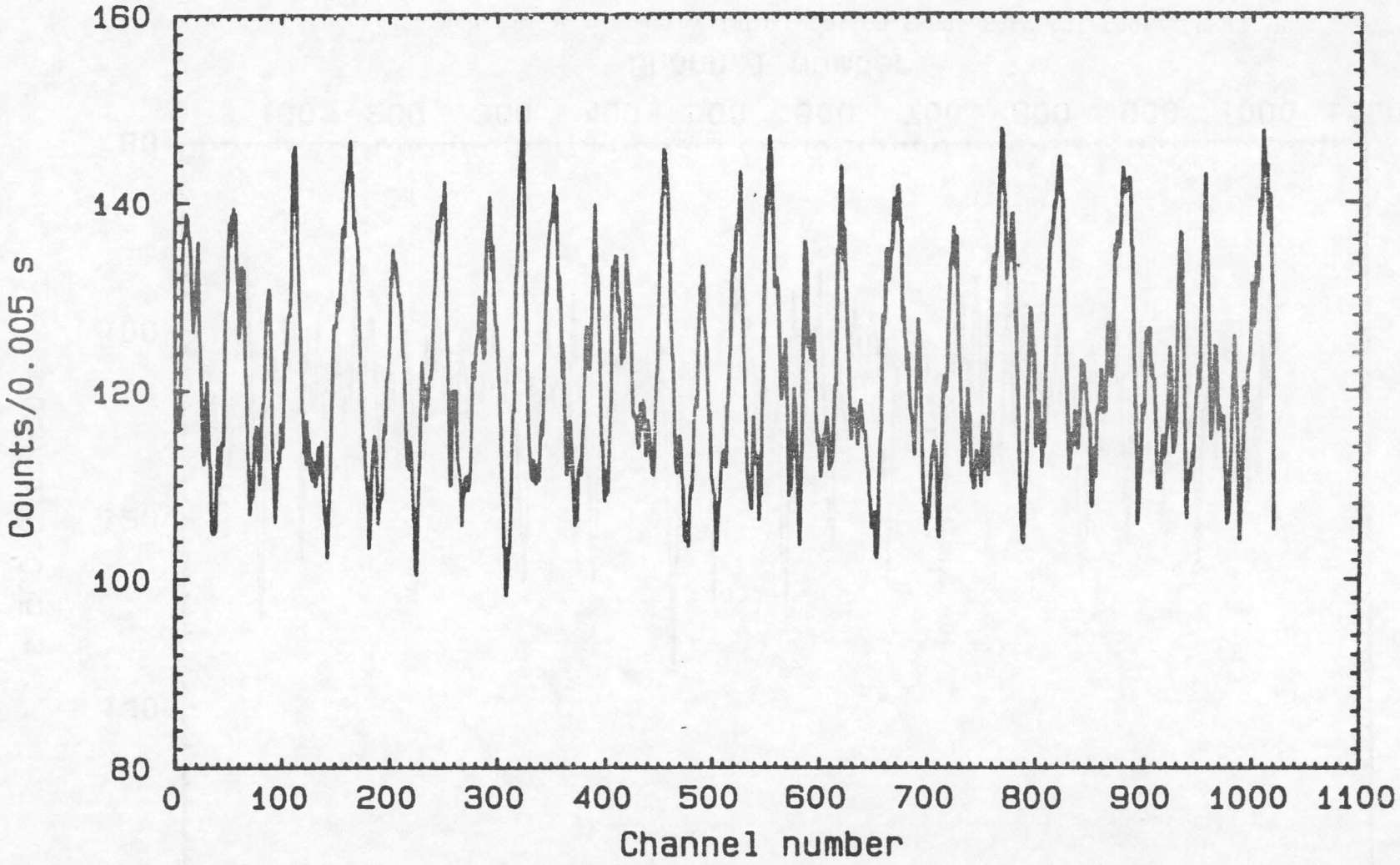

Fig. 6 - Smoothed histogram of gamma-ray interrogation count rate for slug flow shown in Fig. 2c

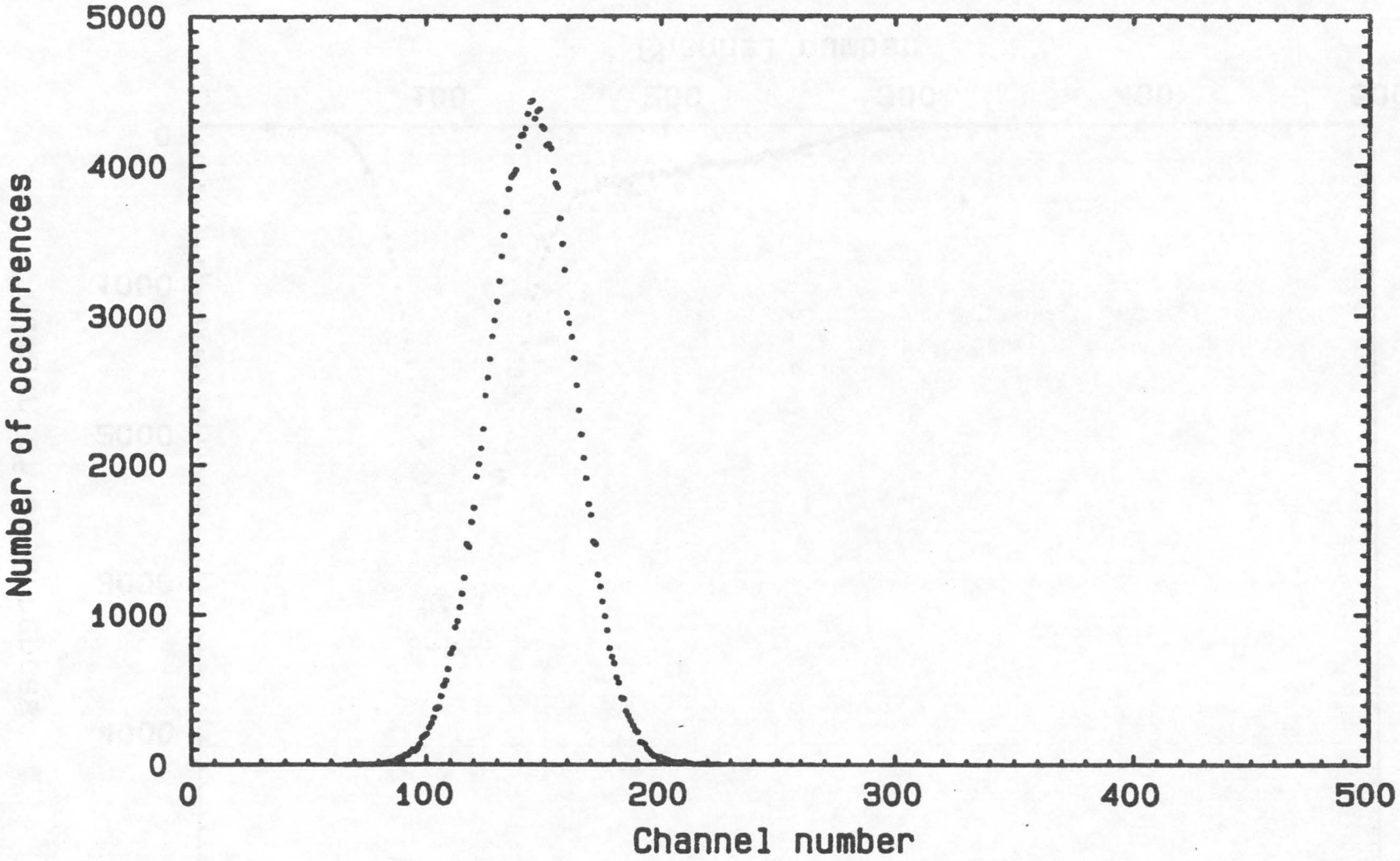

Fig. 7 - Un-normalized PDD function observed for fine bubble flow (Fig. 2a) with theortical FWHM

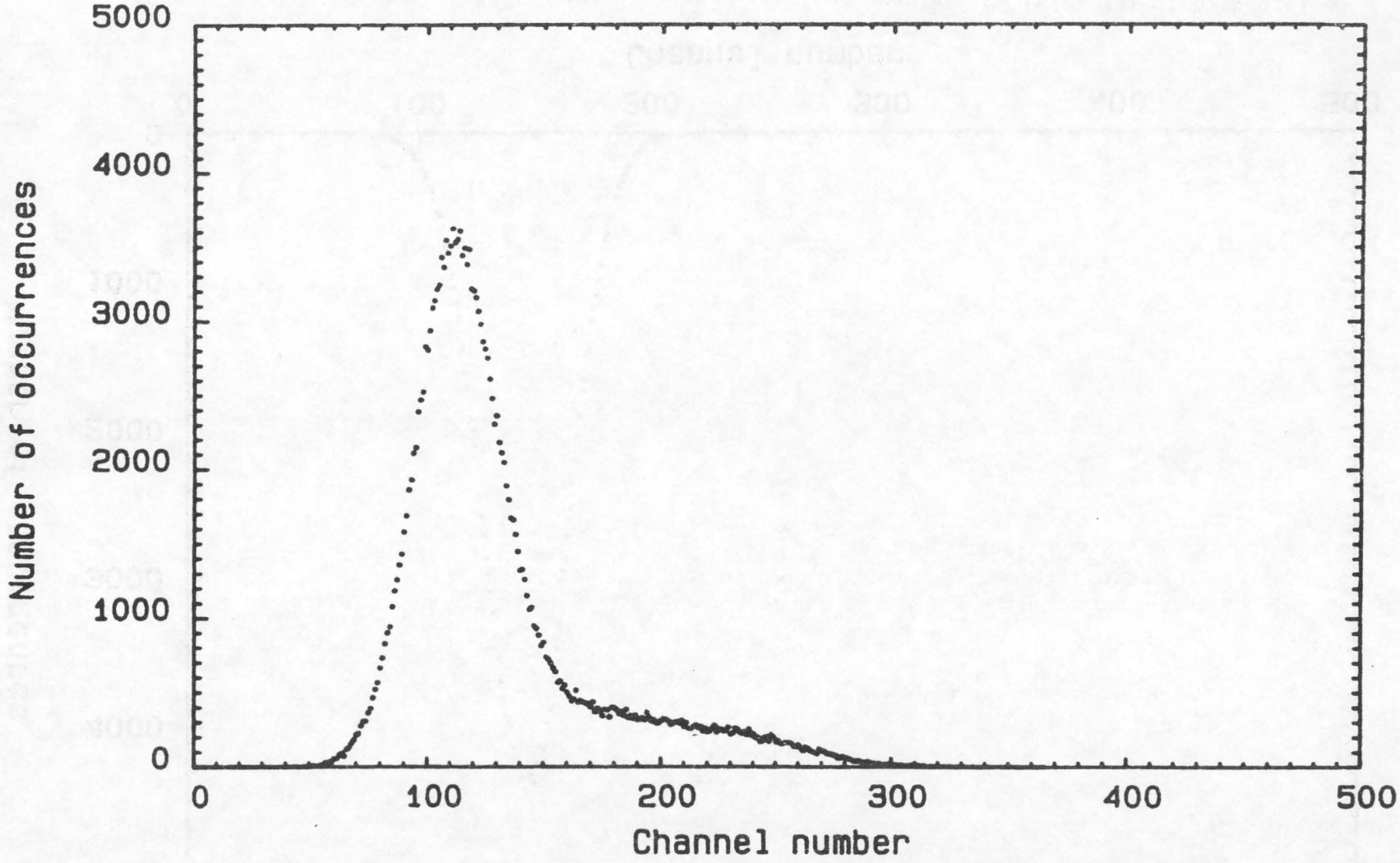

Fig. 8 - Un-normalized PDD function observed for independent bubble flow (Fig. 2b) with tail at high count rate

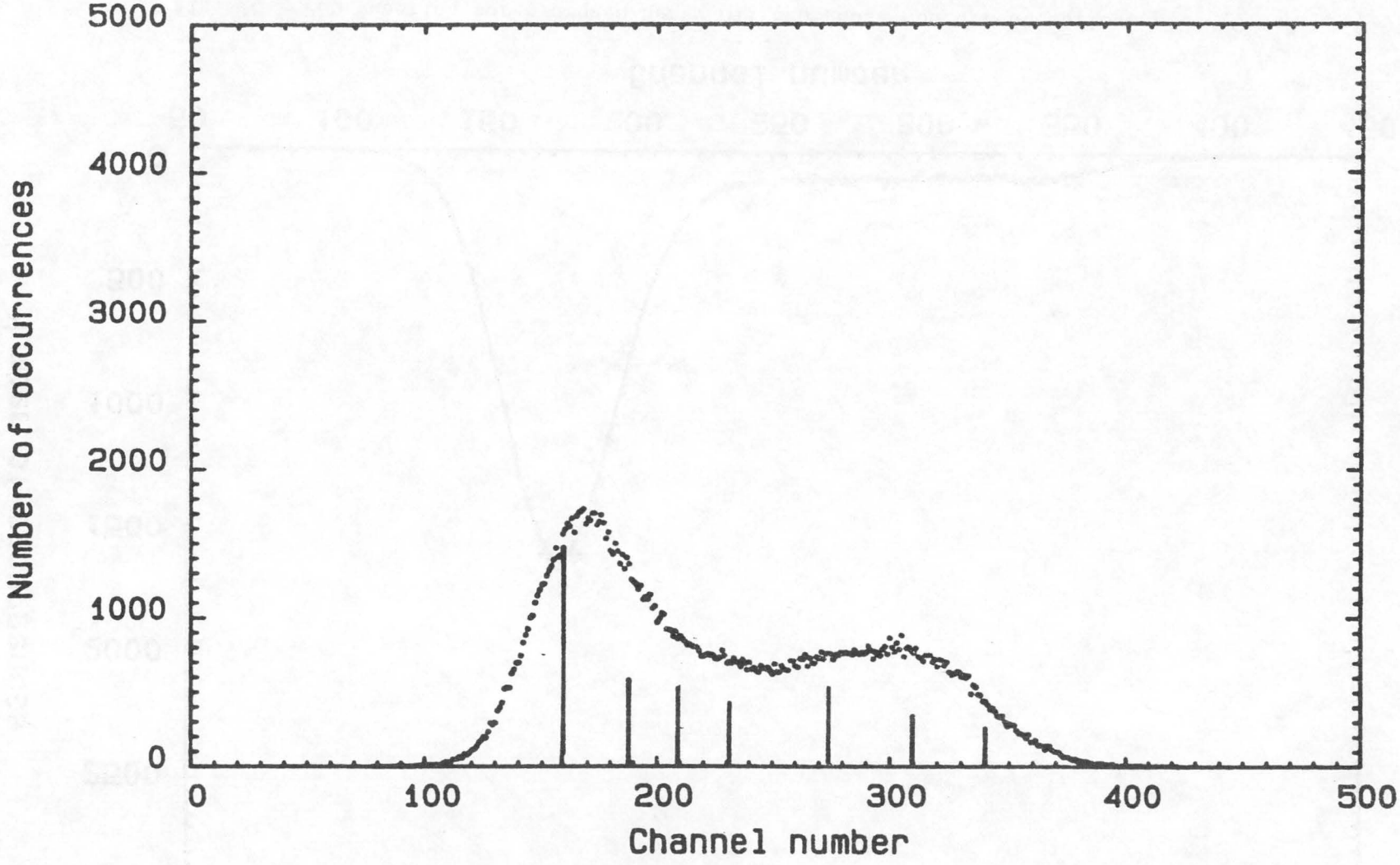

Fig. 9 - Un-normalized PDD function observed for slug flow (Fig. 2c) with distinguished peak at high count rate for gas slugs. Vertical bars are deconvoluted sub-spectra.

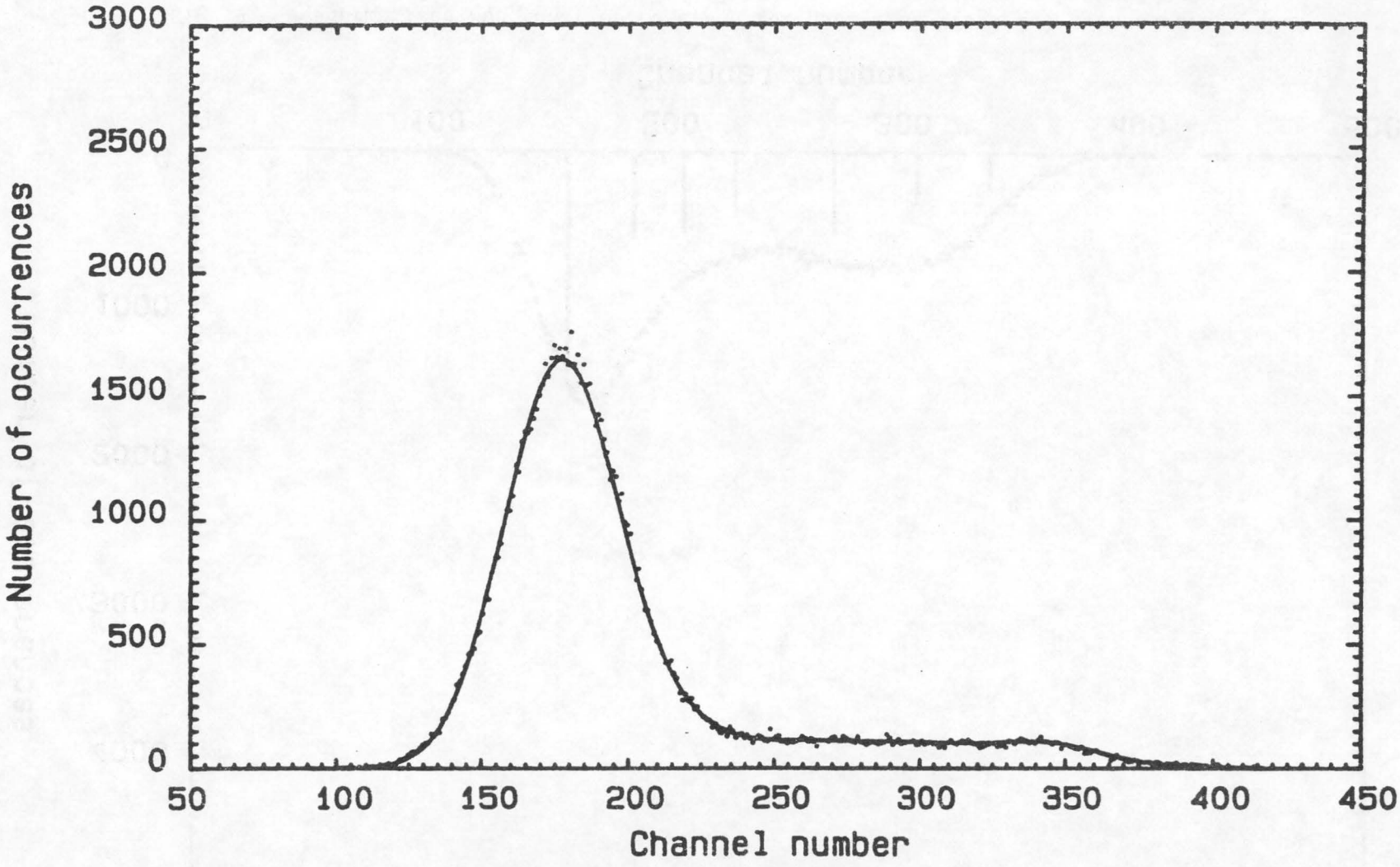

Fig. 10 - PDD function for hydrogen/heavy oil two-phase concurrent upflow at 200°C and 1.38 MPa with superficial gas velocity of 2.02 cm/s

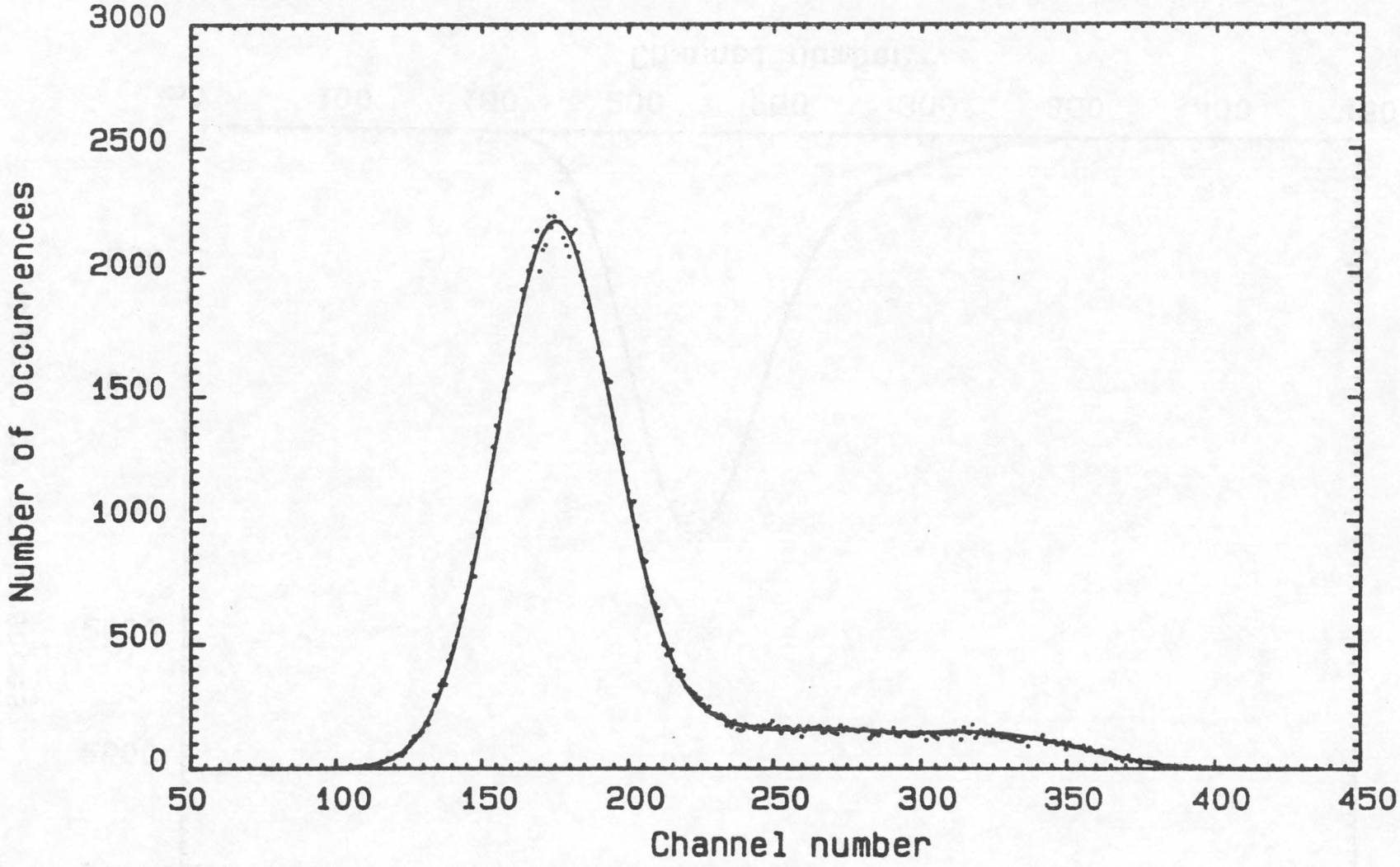

Fig. 11 - PDD function for hydrogen/heavy oil two-phase concurrent upflow at 200°C and 10.35 MPa with superficial gas velocity of 1.66 cm/s

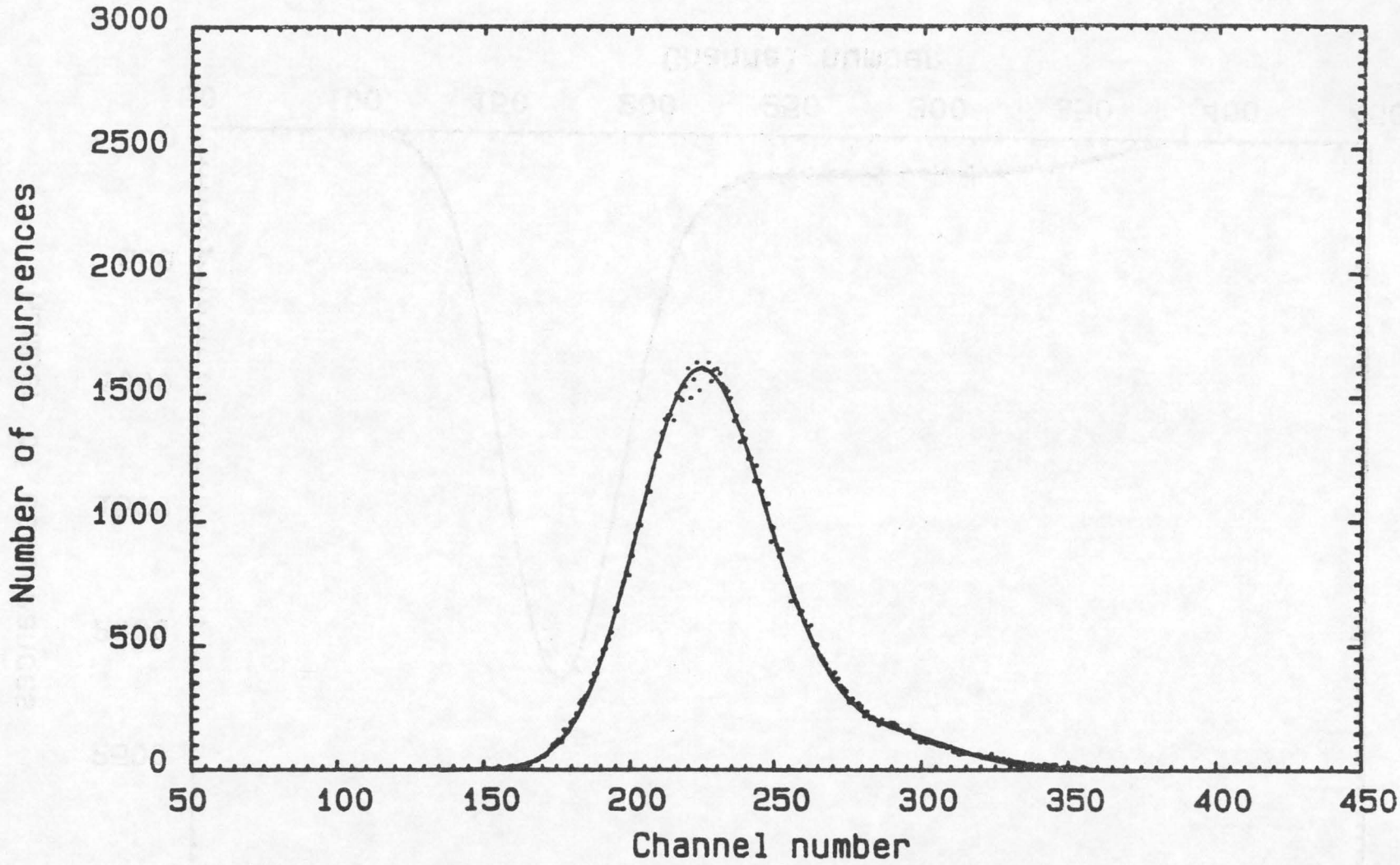

Fig. 12 - PDD function for hydrogen/heavy oil two-phase concurrent upflow at 300°C and 13.79 MPa with superficial gas velcity of 2.47 cm/s

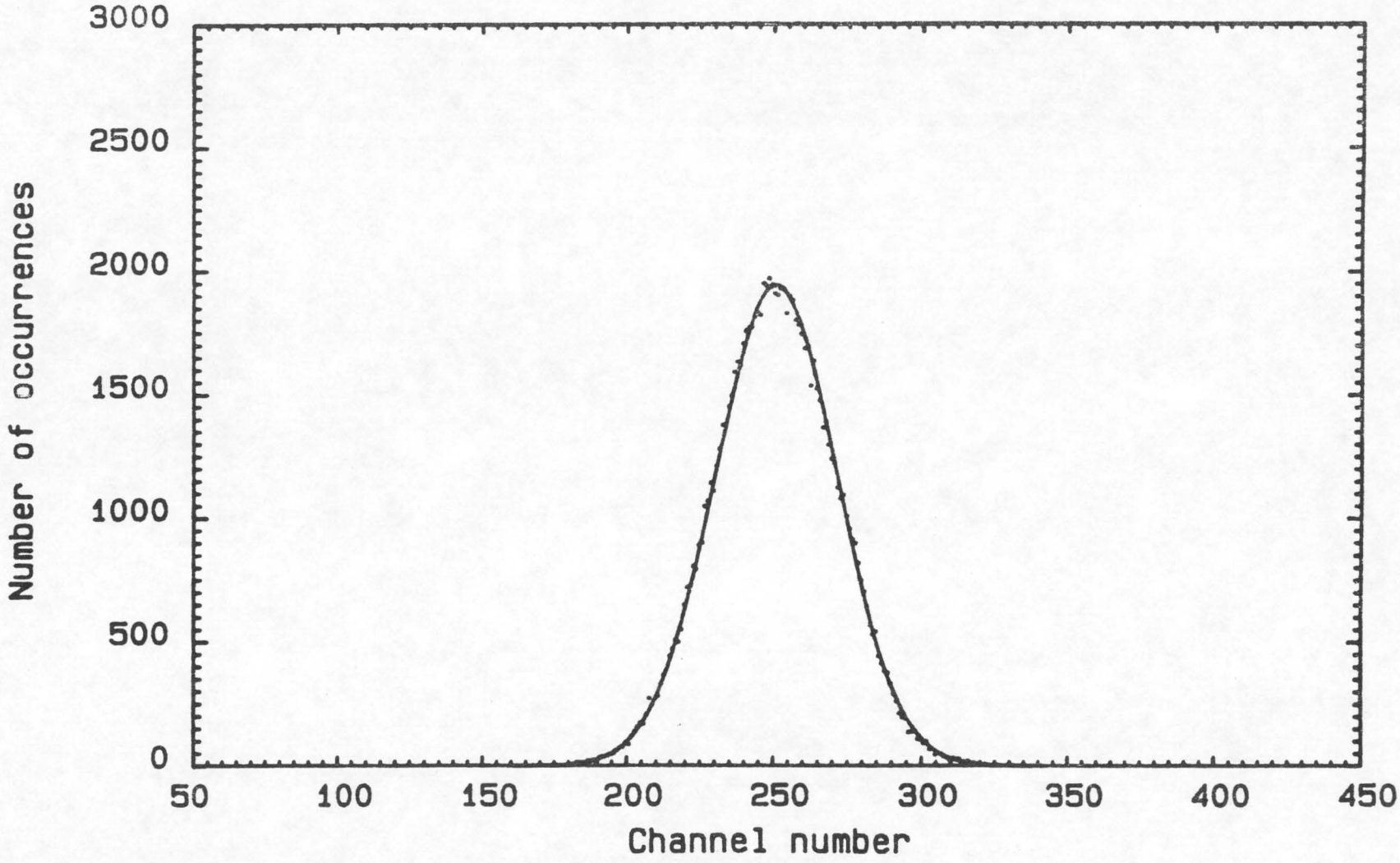

Fig. 13 - PDD function for hydrogen/heavy oil two-phase concurrent upflow at 350°C and 13.75 MPa with superfical gas velocity of 2.19 cm/s